



OPTIMAL SEISMIC DESIGN OF ASYMMETRIC BUILDINGS

Raul BARRON¹ and A. Gustavo AYALA²

SUMMARY

This paper addresses the problem of evaluating and reducing the torsional response of an asymmetric structure when subjected to a seismic excitation modelled by a stochastic process. A procedure of analysis for hysteretic structures is developed based on the equivalent linearization technique and the transfer matrix method. A new proposal for calculating the linearization coefficients is presented. The effectiveness of the procedure is evaluated using a numerical example. It is shown that the procedure provides a good approximation of the torsional response allowing for modifications in design to improve seismic performance.

INTRODUCTION

A rational approach for the seismic design and performance evaluation of asymmetric buildings has to consider the random nature of earthquakes. However, the non-linear behaviour that occurs when a structure undergoes some damage when excited by a strong earthquake makes the random response evaluation difficult. The non-linear response of a structure is hysteretic in nature, *i.e.*, it depends on the history of motion, rather than only on the instantaneous motion. Because of this, analytical studies of random response of inelastic structures have been focussed mostly on the development of approximate methods. Among these methods is the equivalent linearization method proposed first by Caughey [1, 2].

Much of the interest in the equivalent linearization method for practical applications is due to the introduction of a smooth and versatile hysteresis model by Bouc [3] and further developed by Wen [4]. In this model the hysteretic force is included by using an additional state variable controlled by a non-linear first-order differential equation. Assuming a Gaussian distribution for the state variables which control the hysteretic behaviour, close form solutions for the coefficients of the linearized equation were found by Wen [4]. In the original behaviour model the hysteretic variable is bounded by its yield strength, however, the linearized model proposed in this paper assigns probability to the entire state space, so that the obtained results are affected by assumptions on the behaviour of the hysteretic variable in the regions which really should have zero probability. Because of this, divergent solutions have been reported for the smooth model under the Gaussian assumption, Baber and Wen [5].

¹ Professor, Facultad de Ingeniería, Universidad Autónoma de Zacatecas, Zacatecas, Zac, 98000, Mexico.
Email: raul_barron@yahoo.com

² Research Professor, Instituto de Ingeniería, UNAM, Ciudad Universitaria, Mexico D.F. 04510, México.
Email: gayala@dali.fi-p.unam.mx.

The purpose of this paper is to present a new method for calculating the linearization coefficients for the smooth Bouc-Wen model and their incorporation in a numerical procedure for analyzing asymmetric buildings under random ground motions. This method uses the concept of conditional probability to modify the Gaussian probability density function by truncating its tails beyond the yield strength of the restoring force. The procedure is based on a transfer matrix approach as presented by Bo *et al.* [6], incorporating the equivalent linearization method for the analysis of non-linear 3D asymmetric buildings. Some of the previously used methods for the 3D analysis of buildings considered yield surfaces to take into account the 3D behaviour of the structural elements. However, they usually did not take into account yield hardening and were limited to the analysis of small structures since the resulting system of equations was very large. In contrast, the numerical approach proposed in this paper considers the frames as independent elements, takes into account yield hardening and the system of equation is of a workably size allowing the analysis of large multi-storey buildings.

LINEARIZED EQUATION OF MOTION TO MODEL THE NONLINEAR-TORSIONAL RESPONSE OF SHEAR BUILDINGS

The basic assumptions used in this work to model the non-linear-torsional response of buildings are:

1. Rigid floor diaphragms. The building structure is formed by independent plane frames, interconnected by floor diaphragms considered rigid in their own plane.
2. Shear frame. The plane frames are modelled as shear structures with a single resisting element per floor.
3. The mass of the building is lumped at the centres of mass of the floors.

Under these assumptions, the structural response of buildings can be described using only three degrees of freedom per floor: the lateral displacements in the X and Y directions and the torsional rotation θ .

The analysis proceeds floor-by-floor establishing and solving the equation of motion for each floor. The boundary conditions are the ground displacement at the base of the building and the zero shear force at the top. Let $\{u_n\} = \{u_{X_n} \ u_{Y_n} \ \theta_n\}^T$ be the displacement vector of the n^{th} floor relative to the ground and $\{q_n\} = \{q_{X_n} \ q_{Y_n} \ T_n\}^T$ the resultant shear forces in the X , Y and θ directions of the resisting elements below that floor. The state variables of the n^{th} floor are shown in Fig. 1; in which $\{m_n \ddot{u}_{X_n} \ m_n \ddot{u}_{Y_n} \ J_n \ddot{\theta}_n\}^T$ is the vector of inertial forces and $\{q_{X_{n+1}} \ q_{Y_{n+1}} \ T_{n+1}\}^T$ is the vector of resultant shear forces of the upper floor.

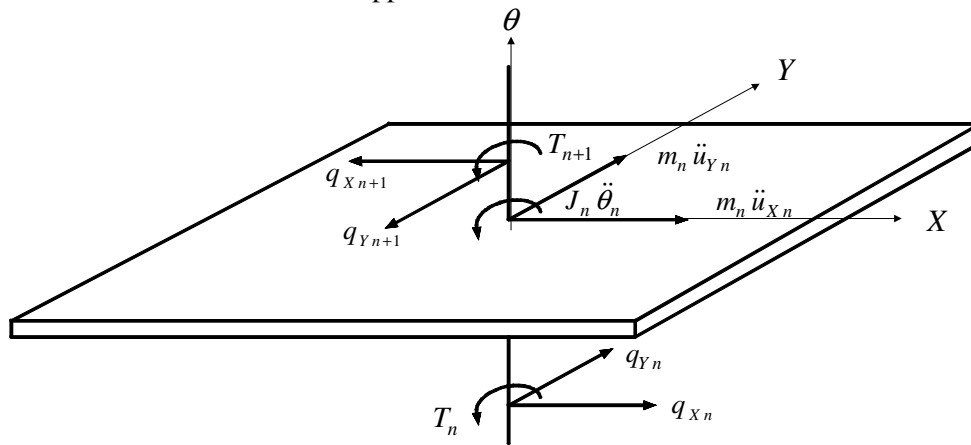


Figure 1. Illustration of state variables at the n^{th} floor.

From the free body diagram illustrated in Fig.1, it is clear that the equation of motion for the n^{th} floor is

$$\begin{bmatrix} m_n & 0 & 0 \\ 0 & m_n & 0 \\ 0 & 0 & J_n \end{bmatrix} \begin{Bmatrix} \ddot{u}_{Xn} \\ \ddot{u}_{Yn} \\ \ddot{\theta}_n \end{Bmatrix} + \begin{Bmatrix} q_{Xn} \\ q_{Yn} \\ T_n \end{Bmatrix} - \begin{Bmatrix} q_{Xn+1} \\ q_{Yn+1} \\ T_{n+1} \end{Bmatrix} = 0 \quad (1)$$

where m_n is the mass and J_n the moment of inertia of the n^{th} floor.

The resultant shear force $\{q_n\}$ is obtained by the summation of the individual shear forces q_{jn} of the resisting elements below the n^{th} floor. The forces q_{jn} represent a combination of three components: a linear viscous damping term, $c_{jn}(v_{jn} - v_{jn-1})$, a linear stiffness term, $\alpha_{jn}k_{jn}(u_{jn} - u_{jn-1})$, and a hysteretic term, $(1 - \alpha_{jn})k_{jn}z_{jn}$, where $0 \leq \alpha_{jn} \leq 1$ is the rigidity ratio, k_{jn} is the initial stiffness, and c_{jn} is the damping coefficient.

The calculation of the relative displacements, $\hat{u}_{jn} = u_{jn} - u_{jn-1}$, and relative velocities, $\hat{v}_{jn} = v_{jn} - v_{jn-1}$, of the resisting elements, requires the projections of the floor displacements $\{u_n\} = \{u_{Xn} \ u_{Yn} \ \theta_n\}^T$ and velocities $\{v_n\} = \{v_{Xn} \ v_{Yn} \ \dot{\theta}_n\}^T$ along the directions of each resisting element as shown in the following equations:

$$u_{jn} = [\cos \varphi_j + \sin \varphi_j + d_{jn}] \begin{Bmatrix} u_{Xn} \\ u_{Yn} \\ \theta_n \end{Bmatrix} \quad \text{and} \quad v_{jn} = [\cos \varphi_j + \sin \varphi_j + d_{jn}] \begin{Bmatrix} v_{Xn} \\ v_{Yn} \\ \dot{\theta}_n \end{Bmatrix} \quad (2)$$

where φ_j is the angle with respect to the X axis of the plane that contains the resisting element and d_{jn} is the minimum distance of that plane to the centre of mass. This distance is positive if the shear force q_{jn} produces a positive contribution to the torsional moment, T_n .

The resultant shear force vector $\{q_n\}$ is obtained from the sum of the projections of the individual shear forces q_{jn} along the X , Y and θ directions,

$$\{q_n\} = [K_n]\{u_n - u_{n-1}\} + [C_n]\{v_n - v_{n-1}\} + [B_n]\{z_n\} \quad (3.a)$$

where

$$K_n = \sum_j \alpha_{jn} k_{jn} \begin{bmatrix} \cos^2 \varphi_j & \cos \varphi_j \sin \varphi_j & d_{jn} \cos \varphi_j \\ \cos \varphi_j \sin \varphi_j & \sin^2 \varphi_j & d_{jn} \sin \varphi_j \\ d_{jn} \cos \varphi_j & d_{jn} \sin \varphi_j & d_{jn}^2 \end{bmatrix} \quad C_n = \sum_j c_{jn} \begin{bmatrix} \cos^2 \varphi_j & \cos \varphi_j \sin \varphi_j & d_{jn} \cos \varphi_j \\ \cos \varphi_j \sin \varphi_j & \sin^2 \varphi_j & d_{jn} \sin \varphi_j \\ d_{jn} \cos \varphi_j & d_{jn} \sin \varphi_j & d_{jn}^2 \end{bmatrix} \quad (3.b)$$

$$\text{The columns in the } [B_n] \text{ matrix are } B_{jn} = (1 - \alpha_{jn})k_{jn} \begin{Bmatrix} \cos \varphi_j \\ \sin \varphi_j \\ d_{jn} \end{Bmatrix} \quad (3.c)$$

The hysteretic variables z_{jn} are modelled by a first-order non-linear differential equation. In this work, the model proposed by Wen [4] is used with a non-degrading stiffness and strength, and anti-symmetric yield strength. This model is given by the following equation:

$$\dot{z}_{jn} = g(\hat{v}_{jn}, z_{jn}) = \hat{v}_{jn} - \beta |\hat{v}_{jn}| |z_{jn}| |z_{jn}|^{m-1} - \gamma \hat{v}_{jn} |z_{jn}|^m \quad (4)$$

where β , γ and m are parameters that control the shape of the hysteresis loop, $\hat{v}_{jn} = v_{jn} - v_{jn-1}$ are the relative-velocities of the resisting elements, and the variables z_{jn} have been normalized to their yield displacements, $u_{y,jn}$.

A linearized approximation of Eq. (4) for the resisting element is

$$\dot{z}_{jn} \approx a_{0jn} + a_{1jn} \hat{u}_{jn} + a_{2jn} \hat{v}_{jn} + a_{3jn} z_{jn} \quad (5)$$

The linearization coefficients $a_{i,jn}$ $i = 0, 1, 2, 3$ can be determined by minimizing the mean square error represented by the difference between the results of the nonlinear model in Eq. (4) and those of the linearized Eq. (5). It has been shown that the only non-zero coefficients are a_{2j} and a_{3j} , Wen [2]. In terms of the linearized Eq. (5), the differential equations for the z_{jn} variables may be written as

$$\{\dot{z}_n\} = [A_{2n}](v_n - v_{n-1}) + [A_{3n}]\{z_n\} \quad (6)$$

where A_{3n} is a diagonal matrix formed with the coefficients a_{3jn} and A_{2n} is a three column matrix containing in each row the terms $a_{2jn} [\cos \varphi_j \quad \sin \varphi_j \quad d_{jn}]$

Considering Eqs. (3.a) and (6), in Eq. (1), gives the equations of motion for the n^{th} floor in terms of the state variables of two consecutive floors. Since $\dot{u}_n = v_n$ these equations can be expressed as a system of first-order differential equations, *i.e.*,

$$\begin{bmatrix} \Delta & -I & 0 \\ 0 & -M_n \Delta & I \\ K_n & C_n & 0 \end{bmatrix} \begin{Bmatrix} u_n \\ v_n \\ q_{n+1} \end{Bmatrix} = \begin{bmatrix} 0 & 0 & 0 \\ 0 & 0 & I \\ K_n & C_n & I \end{bmatrix} \begin{Bmatrix} u_{n-1} \\ v_{n-1} \\ q_n \end{Bmatrix} - \begin{bmatrix} 0 \\ 0 \\ B_n \end{bmatrix} \{z_n\} \quad (7)$$

where I is the 3x3 identity matrix and Δ is a diagonal matrix formed by a first-order differential operator on its diagonal. This operator applied to a vector of variables produces the first derivative of its terms.

The systems of Eqs. (6) and (7) are solved floor-by-floor starting from the first floor. The boundary conditions are those given above. The solution procedure used is given in the next section.

The utilization of the equivalent linearization method is justified from the point of view that among the existing approximate methods for analyzing non-linear structures, the equivalent linearization method is better as it allows an efficient handling of high non-linearities in the modelling of multi-degree-of-freedom systems. It is worth mentioning a remark by Socha and Soong [7], which points out that, contrary to what it is often believed, the equivalent linearization method is not an extension of the Krilov-Bogoliubov (KB) method [8] but that in fact stochastic averaging is much closer, but still inferior to equivalent linearization.

TRANSFER MATRIX FORMULATION FOR THE SOLUTION OF THE LINEARIZED EQUATION

The transfer matrix formulation requires the solution of the system of Eqs. (6) and (7) in the frequency domain; for this it is necessary to calculate the Fourier transform of these equations to obtain

$$\begin{bmatrix} iwI & -I & 0 \\ 0 & -iwM_n & I \\ K_n & C_n & 0 \end{bmatrix} \begin{Bmatrix} U_n \\ V_n \\ Q_{n+1} \end{Bmatrix} = \begin{bmatrix} 0 & 0 & 0 \\ 0 & 0 & I \\ K_n & C_n & I \end{bmatrix} \begin{Bmatrix} U_{n-1} \\ V_{n-1} \\ Q_n \end{Bmatrix} - \begin{bmatrix} 0 \\ 0 \\ B_n \end{bmatrix} \{Z_n\} \quad (8)$$

$$\text{and} \quad [iwI - A_{3n}] \{Z_n\} = [A_{2n}] \{V_n - V_{n-1}\} \quad (9)$$

where the Fourier transforms of the state variables are denoted with capital letters, *i.e.*, U_n, V_n, Q_n, Z_n represent the Fourier transforms of u_n, v_n, q_n, z_n respectively, and $i\omega$ represents the frequency variable with $i = \sqrt{-1}$.

To express the state vector of the n^{th} floor in terms of the state vector of the $(n-1)^{\text{th}}$ floor, Eq. (8) is solved to obtain

$$\begin{Bmatrix} U_n \\ V_n \\ Q_{n+1} \end{Bmatrix} = \begin{bmatrix} D_n^{-1}K_n & D_n^{-1}C_n & D_n^{-1} \\ iwD_n^{-1}K_n & iwD_n^{-1}C_n & iwD_n^{-1} \\ -w^2M_nD_n^{-1}K_n & -w^2M_nD_n^{-1}C_n & I - w^2M_nD_n^{-1} \end{bmatrix} \begin{Bmatrix} U_{n-1} \\ V_{n-1} \\ Q_n \end{Bmatrix} - \begin{bmatrix} D_n^{-1}B_n \\ iwD_n^{-1}B_n \\ -w^2M_nD_n^{-1}B_n \end{bmatrix} \{Z_n\} \quad (10)$$

where $D_n = [K_n + iwC_n]$.

Eq. (10) may be written in a more compact form using the following notation

$$\{\mathbf{U}_n\} = [P] \{\mathbf{U}_{n-1}\} - [B] \{Z_n\} \quad (11)$$

where vector $\{\mathbf{U}_n\} = \{U_n \ V_n \ Q_{n+1}\}^T$ contains the state variables of the n^{th} floor.

Substituting $\{V_n\}$ of Eq. (10) in Eq. (9) and dividing by $i\omega$, the following equation expressing $\{Z_n\}$ in terms of the response variables of the $(n-1)^{\text{th}}$ floor is obtained

$$\left[I - (iw)^{-1}A_{3n} + D_n^{-1}B_n \right] \{Z_n\} = A_{2n} \left[D_n^{-1}K_n \quad D_n^{-1}C_n - (iw)^{-1} \quad D_n^{-1} \right] \begin{Bmatrix} U_{n-1} \\ V_{n-1} \\ Q_n \end{Bmatrix} \quad (12)$$

which may be written in a more compact form using the following notation:

$$[E_n] \{Z_n\} = [G_n] \{\mathbf{U}_{n-1}\} \quad (13)$$

Solving for $\{Z_n\}$ and substituting it in Eq. (11) allows $\{\mathbf{U}_n\}$ to be expressed in terms of $\{\mathbf{U}_{n-1}\}$ as:

$$\{\mathbf{U}_n\} = [P_n] \{\mathbf{U}_{n-1}\} - [E_n^{-1}G_nB_n] \{\mathbf{U}_{n-1}\} \quad \text{or} \quad \{\mathbf{U}_n\} = [H_n] \{\mathbf{U}_{n-1}\} \quad (14)$$

where $[H_n] = [P_n - E_n^{-1}G_nB_n]$ is the transfer matrix of the n^{th} floor.

Special attention is needed in deriving the transfer matrix between the ground and the first floor, which is given as the transfer relationship between the ground acceleration and the first floor state variables. The equations for the first floor are:

$$\begin{bmatrix} iw & -I & 0 \\ 0 & -iwM_1 & I \\ K_1 & C_1 & 0 \end{bmatrix} \begin{Bmatrix} U_1 \\ V_1 \\ Q_2 \end{Bmatrix} = \begin{bmatrix} 0 & 0 & 0 \\ 0 & 0 & I \\ (iw)^{-2}K_1 & (iw)^{-1}C_1 & I \end{bmatrix} \begin{Bmatrix} \ddot{U}_0 \\ \ddot{U}_0 \\ Q_1 \end{Bmatrix} - \begin{bmatrix} 0 \\ 0 \\ B_1 \end{bmatrix} \{Z_1\} \quad (15)$$

$$[iwI - A_{3_1}] \{Z_1\} = [A_{2_1}] \{V_1 - (iw)^{-1} \ddot{U}_0\} \quad (16)$$

where \ddot{U}_0 is a diagonal matrix containing the Fourier transforms of the three components of the ground acceleration, along the X , Y , and θ directions; and Q_1 is a diagonal matrix containing the base shear for each component of the ground acceleration.

Following the same procedure as that used to derive the transfer matrix of the n^{th} floor, the transfer matrix of the first floor may be derived relating $\{U_1\}$ with $\{U_0\}$, that is

$$\{U_1\} = [H_1] \{U_0\} \quad (17)$$

Having calculated the transfer matrices of all floors, the state variables of the n^{th} floor can be related to the ground state variables as

$$\{U_n\} = [H_n H_{n-1} \cdots H_1] \{U_0\} = [T_n] \{U_0\} \quad (18)$$

The base shear is calculated by introducing the assumed boundary conditions in the equation for the top floor. For this, it is assumed that the ground acceleration in each of the three components is a Dirac delta function, *i.e.*, its Fourier transform is equal to one. Then, the state variables $\{u_n\} = \{u_n \ v_n \ q_n\}^T$ are the impulse response functions and their Fourier transforms $\{U_n\} = \{U_n \ V_n \ Q_{n+1}\}^T$ are the frequency response functions. Thus, the equation for the top floor with the appropriated boundary conditions is

$$\begin{Bmatrix} U_N \\ V_N \\ 0 \end{Bmatrix} = [T_N] \begin{Bmatrix} I \\ I \\ Q_1 \end{Bmatrix} \quad (19)$$

where I is the 3x3 identity matrix and 0 is a 3x3 matrix of zeros and Q_1 represents a 3x3 matrix where each column contains the base shear for each component of the ground acceleration.

In this study, the torsional ground acceleration was ignored; therefore the base shear Q_1 has only two columns and there are only two frequency-response functions for each response variable. Thus, for example, to find the variance of the displacement of the n^{th} floor in the X direction, $\sigma_{u_{nX}}^2$, requires the evaluation of the following integral

$$\sigma_{u_{nX}}^2 = \int_{-\infty}^{\infty} [U_{nXX} \ U_{nXY}] \begin{bmatrix} S_{\ddot{X}\ddot{X}} & S_{\ddot{X}\ddot{Y}} \\ S_{\ddot{Y}\ddot{X}} & S_{\ddot{Y}\ddot{Y}} \end{bmatrix} \begin{Bmatrix} \overline{U_{nXX}} \\ \overline{U_{nXY}} \end{Bmatrix} d\omega \quad (20)$$

where $U_{XX,n}$ and $U_{XY,n}$ are the frequency response functions of the displacement u_{nX} for the X and Y components of the ground acceleration, respectively, \bar{U} is the conjugate function of U , and $[S]$ is a matrix containing the auto- and cross-spectral density functions of the ground acceleration.

Evaluation of the linearization coefficients using the conditional probability concept

In this subsection, an alternative procedure to calculate the linearization coefficients is presented. This procedure uses a modified Gaussian probability density function (pdf) result of truncating its tails beyond the yield strength of the resisting force. Procedures that truncate the tails of the Gaussian pdf have been used before, e.g. Kimura *et al.* [9] proposed the use of a truncated Gaussian density combined with Dirac pulses to simulate the effect of the concentration at the maximum values of the hysteretic component of bilinear systems. On the other hand, the procedure here presented distributes the contribution of the truncated tails uniformly in the truncated pdf. Both methods are approximate ways of introducing the contribution of the inelastic response; the concentrated pdfs presume highly inelastic behaviour, whereas the distributed one considers a less severe inelastic behaviour corresponding, approximately, to mean ductility demands between 1 and 4. In the application of the suggested procedure, the Bouc-Wen model is used; with this model the linearization coefficients may be expressed in almost closed form with one simple integral needing to be evaluated numerically.

Considering the domain of definition of z_j , *i.e.*, $-1 \leq z_j \leq 1$, the following conditional probability provides the probability distribution of the state variables (\hat{v}_j, z_j) , where \hat{v}_j is the relative velocity and the variable z_j has been normalized to its yield displacement, u_y .

$$\begin{aligned} P(\hat{v}_j \leq v \cap z_j \leq z \mid -1 \leq z_j \leq 1) &= 0 \quad z_j < -1 \\ &= \frac{1}{c} \int_{-1}^z \int_{-\infty}^v f_{\hat{v}_j z_j}(\hat{v}_j, z_j) d\hat{v}_j dz_j \quad -1 \leq z_j \leq 1 \\ &= 1 \quad z_j > 1 \end{aligned} \quad (21)$$

where $c = \int_{-1}^1 \int_{-\infty}^{\infty} f_{\hat{v}_j z_j}(\hat{v}_j, z_j) d\hat{v}_j dz_j = \text{erf}(1/\sqrt{2}/\sigma_z)$, and $\text{erf}(\cdot)$ is the error function.

The modified density function $f_{\hat{v}_j z_j}(\hat{v}_j, z_j \mid -1 \leq z_j \leq 1)$ of the state variables (\hat{v}_j, z_j) is obtained by differentiating Eq. (21) to give

$$\begin{aligned} f_{\hat{v}_j z_j}(\hat{v}_j, z_j \mid -1 \leq z_j \leq 1) &= \frac{1}{c} f_{\hat{v}_j z_j}(\hat{v}_j, z_j) \quad -\infty < \hat{v}_j < \infty \quad -1 \leq z_j \leq 1 \\ &= 0 \quad \text{elsewhere} \end{aligned} \quad (22)$$

The linearization of the non-linear model in Eq. (4) requires minimizing the mean square error between this equation and the linearized Eq. (5). Since the non-linear model does not depend on the relative displacement of the element, \hat{u}_j , and the response is a zero-mean process, the coefficients a_{0j} and a_{1j} are zero; therefore the equation to minimize is

$$\mathcal{E}^2 = (g(\hat{v}_j, z_j) - (a_{2j}\hat{v}_j + a_{3j}z_j))^2 \quad (23)$$

Since the behaviour of the resisting elements depends only upon the relative coordinates between adjacent nodes, it may be shown that each element can be linearized individually, Roberts and Spanos [10]. Minimizing the mean square error, \mathcal{E}^2 , gives the following condition

$$\frac{\partial}{\partial a_i} E\{\mathcal{E}^2\} = E\left\{2\mathcal{E} \frac{\partial \mathcal{E}}{\partial a_i}\right\} = 0 \quad (24)$$

Substituting Eq. (23) in Eq. (24) gives

$$[\Gamma] \begin{Bmatrix} a_{2j} \\ a_{3j} \end{Bmatrix} = E \begin{Bmatrix} \hat{v}_j g \\ z_j g \end{Bmatrix} \quad (25)$$

where $[\Gamma]$ is the covariance matrix of the state variables (\hat{v}_j, z_j) .

Using the modified Gaussian distribution in Eq. (22) to evaluate the expectations, the coefficients a_{2j} and a_{3j} can be determined. For example, the coefficient a_{2j} may be written as

$$a_{2j} = \sum_{k=1}^2 \Gamma_{1k}^{-1} \int_{-1}^{\infty} \int_{-\infty}^{\infty} V g \frac{\exp(-\frac{1}{2} V^T \Gamma^{-1} V)}{2\pi |\Gamma|^{1/2} c} d\hat{v}_j dz_j \quad (26)$$

where $V = \{\hat{v}_j, z_j\}^T$ and $c = \text{erf}(1/\sqrt{2}/\sigma_z)$. Considering that

$$\sum_{k=1}^2 \Gamma_{1k}^{-1} V g \frac{\exp(-\frac{1}{2} V^T \Gamma^{-1} V)}{2\pi |\Gamma|^{1/2}} = -\frac{\partial}{\partial \hat{v}_j} \frac{\exp(-\frac{1}{2} V^T \Gamma^{-1} V)}{2\pi |\Gamma|^{1/2}} \quad (27)$$

Eq (26) can be integrated by parts with respect to \hat{v}_j , and by considering that $\exp(-\frac{1}{2} V^T \Gamma^{-1} V)$ vanishes as $\hat{v}_j \rightarrow \infty$, this integration yields

$$a_{2j} = E \left\{ \frac{\partial}{\partial \hat{v}_j} g(\hat{v}_j, z_j) \right\} \quad (28)$$

The property for the Gaussian distribution shown in Eq. (27) was apparently first introduced by Kozakov [11] on his studies on statistical linearization; however, it is often associated with the names of Atalik and Utku [12], who first applied it to the equivalent linearization method. However, a different result is obtained for the a_{3j} coefficient since the domain of definition of z_j is $-1 \leq z_j \leq 1$ and the term $\exp(-\frac{1}{2} V^T \Gamma^{-1} V)$ does not vanish when $|z_j| = 1$. Following the same procedure of integrating by parts, the next equation is obtained

$$a_{3j} = E \left\{ \frac{\partial}{\partial z_j} g(\hat{v}_j, z_j) \right\} - C \quad (29)$$

where the correction term C is evaluated with the following equation that is written in terms of the adjusted Gaussian pdf in Eq. (22)

$$C = \int_{-\infty}^{\infty} g(\hat{v}_j, 1) f_{\hat{v}_j z_j}(\hat{v}_j, 1) d\hat{v}_j - \int_{-\infty}^{\infty} g(\hat{v}_j, -1) f_{\hat{v}_j z_j}(\hat{v}_j, -1) d\hat{v}_j \quad (30)$$

Substituting the nonlinear function given in Eq. (4) and calculating the derivatives, the following equations are obtained:

$$a_{2j} = E \left\{ \frac{\partial g}{\partial \hat{v}_j} \right\} = E \left\{ 1 - \beta \operatorname{sig}(\hat{v}_j) z_j | z_j |^{m-1} - \gamma | z_j |^m \right\} = 1 - E_1 - E_2 \quad (31)$$

$$a_{3j} = E \left\{ \frac{\partial g}{\partial z_j} \right\} = E \left\{ -\beta m | \hat{v}_j | | z_j |^{m-1} - \gamma m \hat{v}_j | z_j |^{m-1} \right\} = -E_3 - E_4 \quad (32)$$

Taking $\beta = \gamma = 1/2$ and $m = 3$, the following values for the expectations E_i , $i = 1, 2, 3, 4$ are found

$$\begin{aligned} E_1 &= 3I c_0 & E_2 &= 3\sigma_Z A c_0 \\ E_3 &= 3\sigma_V (B + \rho I / \sigma_Z) c_0 & E_4 &= 3\rho \sigma_V A c_0 \end{aligned} \quad (33)$$

$$\text{where } c_0 = \frac{1}{\sqrt{2\pi} \operatorname{erf}(1/\sqrt{2}/\sigma_Z)} \quad A = 2\sigma_Z^2 - (1 + 2\sigma_Z^2) \exp\left(-\frac{1}{2\sigma_Z^2}\right) \quad (34)$$

$$I = \int_0^1 \frac{z^3}{\sigma_Z} \exp\left(-\frac{z^2}{2\sigma_Z^2}\right) \operatorname{erf}\left(\frac{\rho z}{\sqrt{2}\sigma_Z \sqrt{1-\rho^2}}\right) dz \quad (35)$$

$$B = \sigma_Z (1-\rho^2)^2 \left[\sigma_Z \operatorname{erf}\left(\frac{1}{\sqrt{2}\sigma_Z \sqrt{1-\rho^2}}\right) - \frac{1}{\sqrt{1-\rho^2}} \sqrt{\frac{2}{\pi}} \exp\left(-\frac{1}{2\sigma_Z^2(1-\rho^2)}\right) \right] \quad (36)$$

and the correction term C in Eq. (29) is

$$C = c_0 \frac{\sigma_V}{\sigma_Z^2} \left(\rho \exp\left(\frac{-1}{2\sigma_Z^2}\right) \left(1 - \operatorname{erf}\left(\frac{\rho}{\sqrt{2}\sigma_Z \sqrt{1-\rho^2}}\right) \right) - \sqrt{\frac{2}{\pi}} \sigma_Z \sqrt{1-\rho^2} \exp\left(\frac{-1}{2(1-\rho^2)\sigma_Z^2}\right) \right) \quad (37)$$

It is important to notice that the suggested procedure of analysis requires the evaluation of matrices A_{2n} and A_{3n} (see Eq. (12)), which are formed with the linearization coefficients a_{2j} and a_{3j} . However, as seen in Eqs. (31) to (33), these are functions of the response statistics of the element variables, \hat{v}_j and z_j . Therefore, Eqs. (12), (31) and (32) are, in general, a system of highly non-linear algebraic equations in the unknowns, requiring for their solution an iterative procedure. In this study, the next iterative procedure is used:

- (a) Obtain the initial values of the response statistics assuming the linearization coefficients: $a_{2j} = 1$ and $a_{3j} = 0$. These values correspond to a linear-elastic analysis as the hysteretic variables have zero contribution.
- (b) Calculate new values of the linearization coefficients.
- (c) Obtain revised values of the response statistics from a new analysis.
- (d) Repeat steps (b) and (c) until a specified degree of accuracy is reached.

NUMERICAL EXAMPLE

To illustrate the application of the proposed procedure of stochastic analysis of buildings a numerical example is presented. This procedure gives the variances of the response variables used in to obtain the strengths of the resisting elements necessary to produce equal ductility demands in these elements. The example structure is a six-storey reinforced concrete building with four frames in each orthogonal direction and storey heights of 3 m. Fig. 2 illustrates the location of the frames in a typical floor plant of the building. The structural properties of the elements in the building are listed in Table 1.

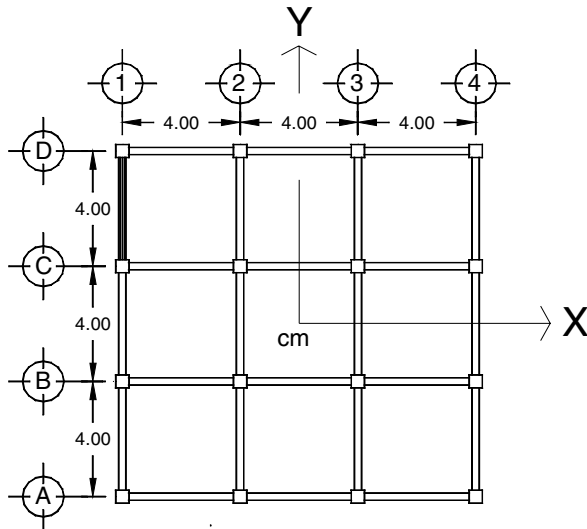


Figure 2. Typical Floor plan of the example building.

Table 1. Structural properties of beams, columns and shear wall

Floor	Columns base x height (cm)	Beams base x height (cm)	Wall Inertia (m ⁴)	Wall Shear area (m ⁴)
4 - 6	40x40	25x40	1.79	0.477
1 - 3	45x45	25x45	2.11	0.482

All frames have the same cross sections and dimensions, except Frame 1, which has a shear wall between axes A and B. The shear wall was modelled as a wide column with properties referred to its centreline. Since the wall is attached to the adjacent columns, the flexural and shear area of the wall were calculated considering the cross-sections of the wall and the two columns. Young's modulus of the concrete in all frames was assumed equal to 6×10^6 N/m and to evaluate the shear deformations in the wall a Poisson ratio of 0.17 was used. The mass of the building was assumed lumped at the centres of mass of the floors. The masses and moments of inertia are listed in Table 2.

Table 2. Translational and rotational floor masses

Floor	Translational Mass (10 ³ kg)	Rotational Mass (10 ³ kg-m ²)
6	186	4805
1, 2, 3, 4, 5	265	6846

To evaluate the storey stiffness of the frames, the building, modelled as a 3D structure with rigid floor diaphragms, was pushed with lateral forces functions of the first and second modes of vibration. The lateral stiffness of frame j in the n^{th} storey was evaluated using the following equation: $K_{nj} = V_{nj} / \Delta_{nj}$ where V_{nj} is the storey shear force and Δ_{nj} the corresponding storey drift. Table 3 lists the calculated stiffnesses. The damping, modelled as structural in the first mode, was 5% of the critical.

Table 3. Storey stiffness of the frames

Frame stiffness in kN/cm Frames	Floor					
	1	2	3	4	5	6
1	6091	3202	2239	1653	1111	459
2, 3, 4, A, B, C and D	488	290	264	207	182	144

As seismic demand, seismic excitations typical of the Valley of Mexico with a dominant period of 2 sec were considered. This demand was modelled as a stationary Gaussian process with zero mean. Its auto- and cross-spectral densities were obtained from the records of the horizontal components of the 8.1 Ms magnitude Michoacan earthquake of September 19, 1985. Ground accelerations recorded at the SCT site were considered. The N00W and N90W ground accelerations were assigned to the respective X and Y directions of the model.

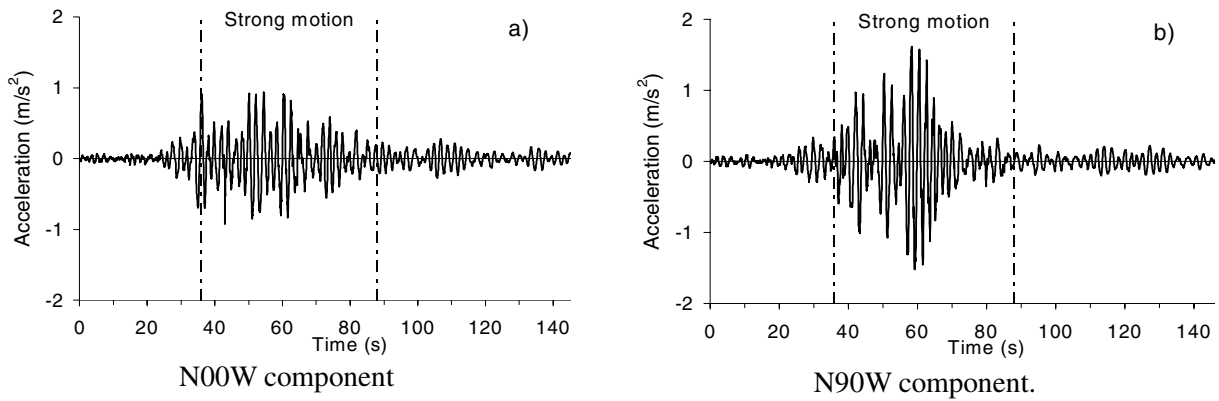


Figure 3. Acceleration time histories of the 9/19/1985 Mexico earthquake recorded at the SCT site.

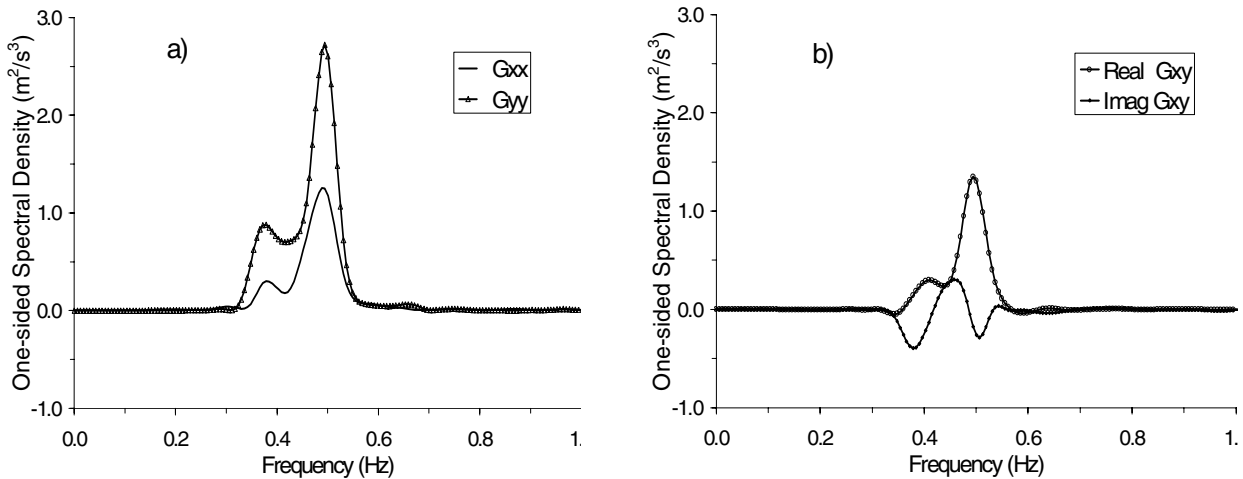


Figure 4. a) auto- and b) cross-spectral density of ground motion.

Fig. 3 shows the strong intensity segments of the records in the X and Y directions corresponding to the 5 to 95% of the total Arias intensity. The duration of these segments was 52 sec. Fig. 4 shows the auto- and cross-spectral densities of these records. These functions were obtained using the MATLAB function *csd*, Krauss *et al.* [13], with a Hamming window of 30 sec. and a 50% overlap which required extending the

length of the records to 60 sec.. The spectral densities were averaged and their intensity scaled to match that corresponding to the strong shaking segment.

PRESENTATION AND ANALYSIS OF RESULTS

Elastic analysis and calculation of the mean elastic force in the resisting elements

The results of the elastic analysis are the standard deviation of the relative displacement, velocity and acceleration for all resisting elements. As example of typical results Fig. 5 presents the standard deviations of the relative displacement of all frames.

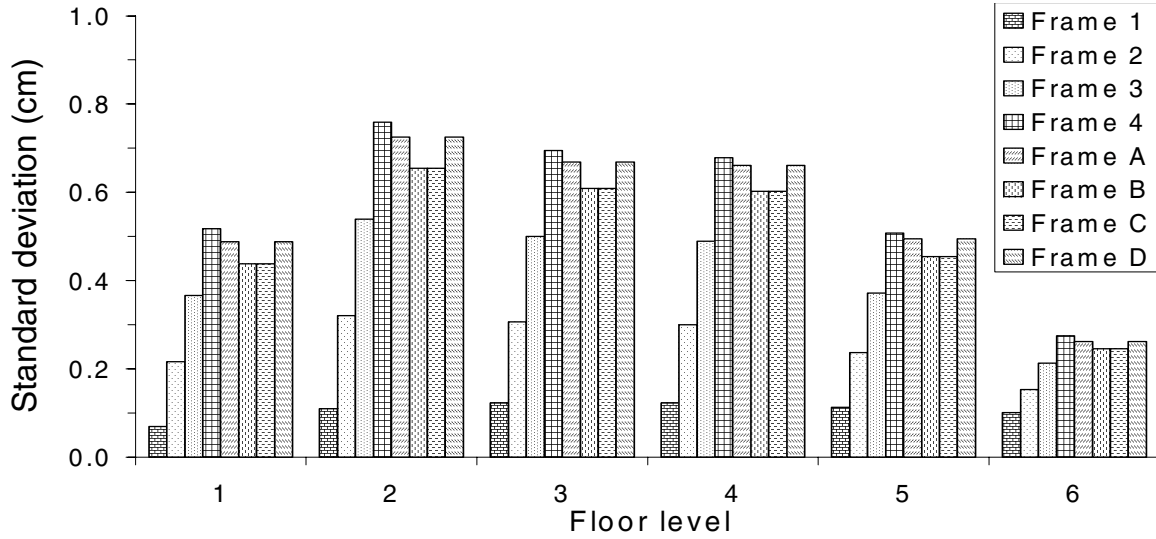


Figure 5. Elastic standard deviation of the relative displacement of the resisting elements.

The maximum response was evaluated using the theory of crossing of random processes. It is well known that for a continuous valued random process, $D(t)$, a peak occurs whenever the velocity is zero, and the acceleration is negative. This suggests that the peak distribution of $D(t)$ can be obtained from the joint distribution of the response vector $\{D(t) V(t) A(t)\}^T$. Using the density function of local maxima derived in Rice [14] (which is the same for local minima) for a zero-mean stationary Gaussian process and assuming that local maxima and minima between successive zero-crossings are independent, the following probability distribution function for the maximum response is obtained, Barron-Corvera [15].

$$F_{D_{\max}}(d) = \left[\Phi\left(\frac{d}{\sigma_D \sqrt{1-\eta^2}}\right) - \eta \Phi\left(\frac{\eta \cdot d}{\sigma_D \sqrt{1-\eta^2}}\right) \exp\left(-\frac{d^2}{2\sigma_D^2}\right) \right]^{N_P} \quad (38.a)$$

$$\text{with } \eta = \frac{\sigma_V^2}{\sigma_D \sigma_A} \quad \text{and} \quad N_P = \frac{1}{\pi} \frac{\sigma_V}{\sigma_D} \cdot t_d \quad (38.b)$$

where $\Phi(\cdot)$ is the standard Normal probability distribution, σ_D , σ_V , σ_A are, respectively, the standard deviation of the displacement, velocity and acceleration. The number of independent peaks and valleys, N_P , is related to the mean rate of zero-crossings and to the strong ground motion duration, t_d .

Using Eq. (38.a), the maximum relative displacement in the resisting elements was evaluated. Fig. 6 illustrates the pdf of the maximum relative-displacement at the base of Frames 1 and 4. This figure shows that Frame 1, which has the shear wall, vibrates within a very short range of displacements as compared with the large range of displacements of Frame 4.

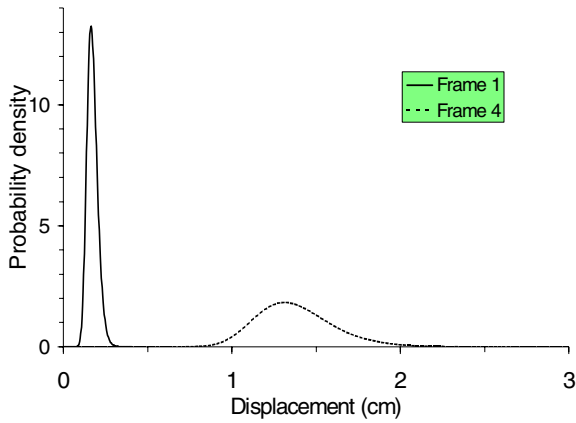


Figure 6. Probability Density functions of maximum elastic displacement, first floor in Frames 1 and 4.

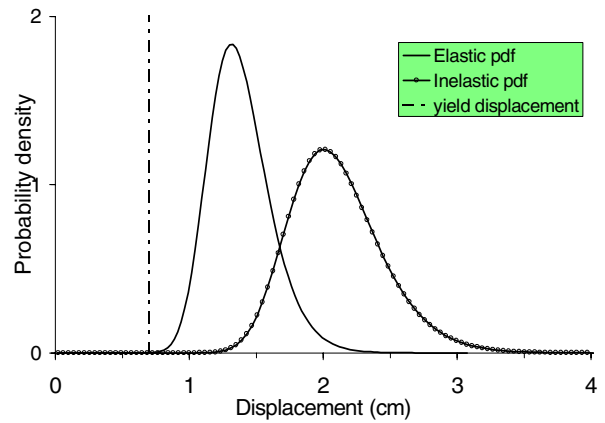


Figure 7 Elastic and inelastic probability density functions of maximum displacement, first floor in Frame 4

With the maximum displacement pdf, the mean maximum displacement in the resisting elements were calculated and used to obtain their elastic mean forces; these were evaluated multiplying the mean displacement of the elements by their stiffnesses. Table 4 presents the calculated elastic forces and the ductilities obtained from the inelastic analysis. The yield strength of the elements was obtained from the elastic forces reduced by a factor of two. This table shows similar ductility demands for all elements, all around 3. Fig. 7 illustrates the pdf of the elastic and inelastic maximum displacement of the first floor in Frame 4. Here, it may be observed that the yielding structure has larger displacements than the elastic structure.

Table 4. Mean elastic force and ductility demand in the inelastic structure.

Floor	Mean Elastic Force (KN)								Ductility							
	1	2	3	4	A	B	C	D	1	2	3	4	A	B	C	D
6	122	58	82	107	104	97	97	104	3.0	3.1	3.1	3.0	3.0	3.0	3.0	3.0
5	327	115	182	250	247	228	228	247	3.0	3.1	3.1	3.0	3.0	3.0	3.0	3.0
4	524	166	273	380	376	345	345	376	3.0	3.1	3.1	3.1	3.0	3.0	3.0	3.0
3	705	216	356	495	484	442	442	484	2.9	3.1	3.1	3.1	3.1	3.0	3.0	3.1
2	896	249	422	594	576	522	522	576	2.9	3.0	3.1	3.1	3.1	3.1	3.1	3.1
1	1071	280	480	678	648	584	584	648	2.9	3.0	3.0	3.0	3.1	3.0	3.0	3.1

Comparison of the ductility demands obtained with the design criterion used above and the design criteria proposed in the Mexican seismic code

To obtain the design elastic forces of the resisting elements, a modal analysis was performed using the first two modes of vibration. The mode shapes and modal frequencies were obtained from the equation of motion that considers the torsional coupling. The first mode has a period of 1.2 sec. and represents pure translation in the X direction. The second mode has a period of 1.1 sec. and corresponds to translations in the Y direction coupled with the rotation of the floors. The generalized single-degree-of-freedom (SDOF) corresponding to the first mode was subjected to the X component of the earthquake excitation (see Fig. 4) and the generalized SDOF corresponding to the second mode was subjected to the Y component. A 5 % damping was assumed for both modes. The calculated shear forces are listed in Table 5 along with the coordinates of the centre of rigidity and centre of mass, and the torsional moments obtained with the design eccentricities proposed in the Mexican code, Eqs. (39).

$$e_1 = 1.5e_s + 0.1b \quad \text{and} \quad e_2 = e_s - 0.1b \quad (39)$$

where e_s is the structural eccentricity and b is the maximum horizontal dimension of the building measured perpendicular to the direction in which the seismic excitation is applied.

Table 5. Storey shear force calculated from the modal analysis, coordinates of the centre of rigidity, centre of mass, and design torsional moments.

Floor	Shear force (kN)		Centre of rigidity (m)		Centre of mass (m)		Torsional moment (kN-m)	
	V _x	V _y	X _{ct}	Y _{ct}	X _{cm}	Y _{cm}	M ₁	M ₂
6	422	324	-1.7	0	0	0	549	824
5	971	746	-3.4	0	0	0	2521	3777
4	1422	1089	-3.8	0	0	0	4179	6269
3	1746	1334	-3.9	0	0	0	5199	7809
2	1942	1481	-4.3	0	0	0	6396	9594
1	2021	1540	-4.5	0	0	0	6877	10310

The shear forces and torsional moments were distributed among the resisting elements. Due to the asymmetry in the Y direction, additional forces were added to the resisting elements in the X direction. As suggested in the Mexican code, 30% of these additional forces were added to the elements in the X direction. Table 6 lists the calculated elastic design forces in the elements. As accepted in the Mexican code, the shear forces obtained from the torsional moments were not subtracted in Frame 1.

Table 6. Elastic design forces in the resisting elements calculated according to the Mexican code and the ductility demand obtained from the inelastic analysis.

Floor	Elastic Force (KN)								Ductility							
	1	2	3	4	A	B	C	D	1	2	3	4	A	B	C	D
6	165	65	81	99	127	120	120	127	2.3	2.7	3.0	3.1	2.2	2.2	2.2	2.2
5	550	113	182	251	302	280	280	302	1.6	3.0	3.0	3.0	2.3	2.3	2.3	2.3
4	871	157	266	375	446	413	413	446	1.6	3.1	3.1	3.1	2.4	2.4	2.4	2.4
3	1078	192	326	461	548	507	507	548	1.7	3.4	3.3	3.3	2.6	2.5	2.5	2.6
2	1283	207	366	526	615	567	567	615	1.9	3.6	3.5	3.5	2.8	2.7	2.7	2.8
1	1364	212	382	551	640	591	591	640	2.2	4.0	3.8	3.9	3.1	3.0	3.0	3.1

The inelastic structure was analyzed and the mean ductility demands in the elements were calculated. Table 6 shows an uneven distribution of ductility demands. Particularly, the elements in the Y direction present larger ductilities than those listed in Table 4.

CONCLUSIONS

A numerical procedure for the non-linear stochastic analysis of asymmetric buildings was presented. The hysteretic restoring force of the resisting elements was modelled using the Bouc-Wen model and a new method for calculating the linearization coefficients. This procedure was used to evaluate the statistics of the response of a six-storey reinforced concrete building subjected to a random ground motion. From the analysis of the obtained results the following conclusions may be draw:

1. Equivalent linearization can effectively be used in the seismic analysis of multi-degree-of-freedom systems representing asymmetric buildings.
2. The proposed procedure for evaluating the linearization coefficients using the modified Gaussian density proved to be very stable when using the Bouc-Wen model with smooth transition coefficients larger than 1.
3. The numerical procedure gives a rational methodology for analyzing asymmetric buildings under random ground motion and it has a great potential in the design of asymmetric buildings.

ACKNOWLEDGMENTS

This research is part the project “Development of Seismic Design Criteria for Torsion” sponsored as a collaboration project between the National Autonomous University of Mexico (UNAM) and the Autonomous University of Zacatecas (UAZ) by the General Directorate for Affairs of the Academic Personnel of UNAM, DGAPA and the Faculty of Engineering of UAZ. Support for this research came also from the National Council for Science and Technology (CONACYT) and the Program for the Improvement of Faculty (PROMEP) of the Ministry of Public Education in Mexico. Their support is gratefully acknowledged. The constructive comments and suggestions of Estebán Flores are appreciated.

REFERENCES

1. Caughey TK. “Response of a nonlinear string to random load.” *J. Appl. Mech.*, 1959; 26: 341-344.
2. Caughey TK. “Equivalent linearization techniques.” *J. Acoust. Soc. Am.*, 1963; 35: 1706-1711.
3. Bouc R. “Forced vibration of mechanical systems with hysteresis.” *Proceedings of the 4th Conference on Non-linear Oscillations*, Prague, 1967.
4. Wen YK. “Method of random vibration of hysteretic systems.” *J. Engineering Mechanics Division, ASCE*, 1976; 102 (EM2): 249-263.
5. Baber TT, Wen YK. “Stochastic equivalent linearization for hysteretic, degrading, multistory structures.” *Dept. of Civil Eng., University of Illinois at Urbana-Champaign, Urbana, ILL*, 1980.
6. Bo W, Ou JP, Soong TT. “Optimal placement of energy dissipation devices for three-dimensional structures.” *Engineering Structures*, 1997; 19(2): 113-125.
7. Socha L, Soong TT. “Linearization in analysis of nonlinear stochastic systems.” in “*Random vibration and fracture mechanics*”, I. Elishakoff (assoc. ed.), *Appl. Mech, Rev*, 1991; 44 (10).
8. Krylov N., Bogoliubov N. “*Introduction to nonlinear mechanics*”. Princeton University Press, New York, 1943.
9. Kimura K, Yasumuro H, Sakata M. “Non-Gaussian equivalent linearization for nonstationary random vibration of hysteretic system.” *Probabilistic Engineering Mechanics*, 1994, 9: 15-22.
10. Roberts JB, Spanos PD. “*Random Vibration and Statistical Linearization*.” John Wiley & Sons, Chichester, New York, 1990.
11. Kazakov IE. “Generalization of the method of statistical linearization to multidimensional systems.” *Automation and Remote Control*, 1965, vol. 26: 1201-1206.
12. Atalik TS, Utku S. “Stochastic linearization of multi-degree-of-freedom non-linear systems.” *Earthquake Engineering and Structural Dynamics*, 1976; vol. 4: 411-420.
13. Krauss TP, Shure L, Little JN. “*Signal processing TOOLBOX – For use with MATLAB*” The MathWorks Inc., Natick, MASS, 1993.
14. Rice SO. “Mathematical analysis of random noise.” *J. Bell System Tech.*, 1944; 23:282-332, 1945; 24:46-156. Reprinted in N. Wax (ed.), *Selected Papers on Noise and Stochastic Processes*, Dover, New York, 1954.
15. Barron-Corvera R. “Spectral evaluation of seismic fragility of structures.” Ph.D. Dissertation, Department of Civil, Structural & Environmental Engineering, State University of New York at Buffalo, Buffalo, N.Y., 2000.